THE JOURNAL OF BIOLOGICAL CHEMISTRY VOL. 289, NO. 42, pp. 29086–29096, October 17, 2014

Escherichia coli D-Malate Dehydrogenase, a Generalist Enzyme Active in the Leucine Biosynthesis Pathway*[S]

Received for publication, July 9, 2014, and in revised form, August 22, 2014 Published, JBC Papers in Press, August 26, 2014, DOI 10.1074/jbc.M114.595363

Anastassia A. Vorobieva[‡], Mohammad Shahneawz Khan[§], and Patrice Soumillion[‡1]

From the [‡]Laboratoire de Biochimie, Biophysique et Génétique des Microorganismes (BBGM), Institut des Sciences de la Vie, Université catholique de Louvain, B-1348 Louvain-la-Neuve, Belgium and the [§]Department of Fisheries, University of Dhaka, Dhaka 1000, Bangladesh

Background: D-Malate dehydrogenase (DmlA) is involved in D-malate catabolism in *Escherichia coli*.
Results: When expressed in the presence of D-malate, DmlA allows growth of a Δ*leuB* strain without leucine.
Conclusion: DmlA physiologically contributes to two core metabolic reactions.
Significance: Several high level activities may coexist in one enzyme and be maintained during the course of evolution.

The enzymes of the β-decarboxylating dehydrogenase superfamily catalyze the oxidative decarboxylation of D-malate-based substrates with various specificities. Here, we show that, in addition to its natural function affording bacterial growth on D-malate as a carbon source, the D-malate dehydrogenase of *Escherichia coli* (*Ec*DmlA) naturally expressed from its chromosomal gene is capable of complementing leucine auxotrophy in a *leuB*$^-$ strain lacking the paralogous isopropylmalate dehydrogenase enzyme. To our knowledge, this is the first example of an enzyme that contributes with a physiologically relevant level of activity to two distinct pathways of the core metabolism while expressed from its chromosomal locus. *Ec*DmlA features relatively high catalytic activity on at least three different substrates (L(+)-tartrate, D-malate, and 3-isopropylmalate). Because of these properties both *in vivo* and *in vitro*, *Ec*DmlA may be defined as a generalist enzyme. Phylogenetic analysis highlights an ancient origin of DmlA, indicating that the enzyme has maintained its generalist character throughout evolution. We discuss the implication of these findings for protein evolution.

It is regularly assumed that superfamilies of enzymes evolved from ancestors featuring broad substrate specificity but low catalytic efficiency. After gene duplication, the redundant copies of the ancestor diverged and specialized to effectively accommodate one substrate and occupy a defined position in a metabolic pathway (1–5). Supporting this evolutionary scenario, modern specialized enzymes frequently retained weak activities on secondary substrates ("substrate promiscuity") or the ability to catalyze secondary reactions ("catalytic promiscuity"), and the secondary activity of one member of the family is often the principal activity of another member of the same family (6–8). Moreover, many enzymes feature secondary activities that are unrelated to their evolutionary history (9–11). In the course of evolution, "promiscuous" activities may be improved to a physiologically relevant level by just a few mutations in the protein and are therefore considered as potential starting points for neofunctionalization (see reviews in Refs. 12–14). For example, one point mutation in the glutamyl phosphate reductase (ProA) enables the enzyme to serve both its original metabolic function and a new one in arginine biosynthesis (15). The mutation increases a promiscuous activity on *N*-acetylglutamyl phosphate by an order of magnitude and results in overexpression of the protein. Overexpression is necessary to simultaneously support both the original and new functions because the mutation had a significant negative effect on the original activity. In some cases, however, the original and promiscuous activities may coexist at a relatively high level in the wild-type enzyme. Genetic complementation of a functional knock-out then only requires protein overexpression (9–11, 16–18). In most of these studies, knock-out complementations were artificially achieved by overexpressing the proteins from multicopy vector systems. Recently, Nam *et al.* (19) estimated that 37% of *Escherichia coli* enzymes are generalists, *i.e.* they promiscuously accept more than one substrate with a relatively high efficiency. By using experimental data to model metabolic networks and fluxes in *E. coli* cells, they found that these generalists can contribute to the catalysis of 65% of the known metabolic reactions while expressed under the control of their natural promoter. These results are significant because enzymes with promiscuous activities on natural metabolites are believed to play an important role in the metabolic plasticity of organisms (20). However, there is no experimental evidence showing that a naturally expressed promiscuous enzyme may simultaneously contribute to more than one metabolic flux *in vivo*.

The superfamily of β-decarboxylating dehydrogenases gathers metabolically important enzymes catalyzing the successive oxidation and decarboxylation of substrates with a common *R*-malate moiety and different γ-substituents on C-3, with various sizes, polarity, or configurations (see Fig. 1). Up to now, five families have been identified: the NAD-dependent isopropylmalate dehydrogenases (IPMDHs),[2] the NAD-dependent isoci-

* This work was supported by a research assistant fellowship from the Belgian Fonds National de la Recherche Scientifique (FNRS) and by Belgian "Inter-university Attraction Poles" Program Project P7/44 iPROS.
[S] This article contains supplemental material.
[1] To whom correspondence should be addressed: Biochimie, Biophysique et Génétique des Microorganismes, Institute of Life Sciences, UCLouvain, Croix du Sud 4–5, Box L7.07.06, B-1348 Louvain-la-Neuve, Belgium. Tel.: 32-1047-3075; Fax: 32-1047-2825; E-mail: patrice.soumillion@uclouvain.be.

[2] The abbreviations used are: IPMDH, isopropylmalate dehydrogenase; IDH, isocitrate dehydrogenase; TDH, tartrate dehydrogenase; HDH, homoisocitrate dehydrogenase; *Pp*, *P. putida*; *Ec*, *E. coli*.

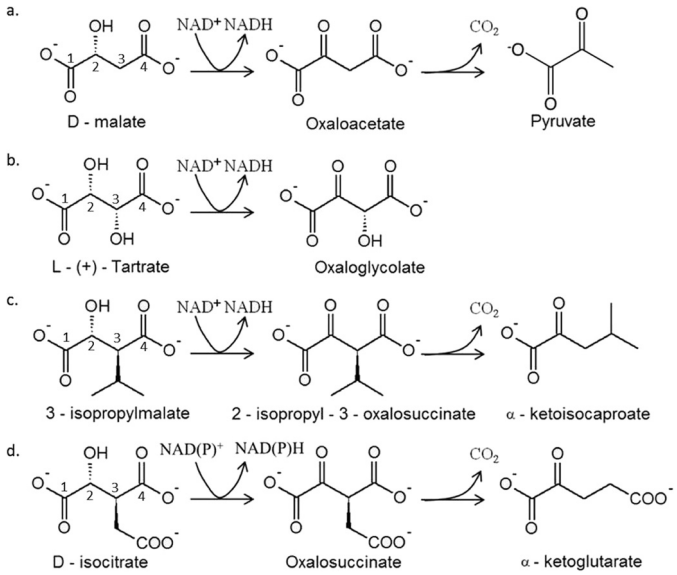

FIGURE 1. **Members of the β-decarboxylating dehydrogenase family catalyze several reactions on D-malate-based substrates.** *a*, *c*, and *d*, oxidative decarboxylation catalyzed by Dml/TDHs, IPMDHs, and NAD(P)-IDHs, respectively. *b*, oxidation described for *Pp*TDH.

trate dehydrogenases (IDHs), the NADP-dependent IDHs, the NAD-dependent D-malate/tartrate dehydrogenases (Dml or TDHs), and the NAD-dependent homoisocitrate dehydrogenases (HDHs). Crystal structures are available for several IDHs (21–23) and IPMDHs (24, 25), for the *Thermus thermophilus* HDH (26), and for the *Pseudomonas putida* TDH (*Pp*TDH) (27). All of them present a conserved dimeric structure. The enzymes of the superfamily are Mg^{2+}- or Mn^{2+}-dependent and share conserved active site residues. They also have very different substrate specificities (see Fig. 1). IPMDHs are specific toward hydrophobic alkyl malate substrates (28), and IDHs exhibit high specificity toward the negatively charged isocitrate (29). In addition to homoisocitrate, the HDH of *Deinococcus radiodurans* also accepts isocitrate and isopropylmalate (30), whereas the HDHs of *T. thermophilus* and *Pyrococcus horikoshii* are active on isocitrate and homoisocitrate only (31, 32). Finally, although *Pp*TDH was first identified as an enzyme supporting growth on L(+)-tartrate, it was later shown to be also active on D-malate and 3-isopropylmalate *in vitro* (33, 34). Although the enzyme transforms both D-malate and 3-isopropylmalate by oxidative decarboxylation, a non-decarboxylating oxidation is observed with L(+)-tartrate (Fig. 1).

In *E. coli*, the D-malate dehydrogenase *Ec*DmlA (*dmlA* gene) with high similarity to *Pp*TDH (76% of identity) is responsible for aerobic growth on D-malate as the sole carbon source (35, 36). It coexists with a paralogous *Ec*IPMDH (*leuB* gene) involved in leucine biosynthesis. It has long been known that *E. coli* strains harboring the *leuB6* genotype produce revertants under leucine starvation conditions (37). However, the fact that most of these revertants are suppressors (*i.e.* no mutation could be detected in the *leuB* locus) indicates that the loss of *Ec*IPMDH can be complemented by another protein (37, 38). In this work, we show that chromosomal expression of *Ec*DmlA affords complementation of the *leuB*$^-$ phenotype when induced by D-malate. The *Ec*DmlA-dependent *leuB*$^+$ phenotype is not observed with glucose. These results are further supported by the biochemical characterization of the purified enzyme, and we discuss its evolutionary implications with the help of a phylogenetic analysis of the superfamily.

EXPERIMENTAL PROCEDURES

Strains and Chemicals—The Δ*leuB* strain HBLB1 was constructed from the HB101 strain using a standard phage P1 transduction protocol (39). The *leuB6* gene was replaced with a kanamycin resistance cassette using the JW5807-2 strain (Δ*leuB*::*kan*) from the Keio Collection (40) as a donor. The cassette insertion was validated by PCR and sequencing.

Cloning—The *dmlA* gene was amplified from the *E. coli* DH12S genome by PCR (Phusion polymerase, Fisher Scientific) and cloned between the NdeI and BamHI sites of the pMal-pIII vector (New England Biolabs) in C-terminal fusion with a GSSG linker and *Strep*-tag II. In the final construct called phDmlA, the *dmlA* gene replaced the entire *malE*-containing ORF and was under the control of the P_{tac} promoter. The genetic construction was verified by sequencing.

Phenotypic Auxotrophy Tests—All phenotypic tests were performed on amino acid-free EZ Rich defined medium. The medium was prepared as described by Neidhardt *et al.* (41), and the 10× EZ solution used to prepare the medium was purchased from Teknova (Hollister, California). For solid medium culture, the medium was solidified with 1.5% agar. The carbon sources were added up to 0.1% (D-glucose) or 0.15% (D-malate), and leucine was used at 1 mM if specified. Proline (1 mM) was added to the culture medium to support growth of the HBLB1 strain. Liquid cultures (100 ml) were inoculated from an overnight preculture of HBLB1 cells preliminary washed with M9 buffer. $CaCO_3$ (10 mM) was added to the medium to reduce the lag time as described (41). Despite this step, a lag time of ~16 h was observed. The cells were inoculated at an initial A_{600} of 0.05 and incubated overnight at 37 °C and 180 rpm. Growth was monitored the next day. For growth tests on solid medium, precultures grown overnight at 37 °C and 180 rpm in LB/kanamycin (50 μg/ml) were harvested by centrifugation and resuspended in 3 ml of M9 buffer. The cells were then sequentially diluted in M9 buffer up to 10^{-5}-fold. 10 μl of each dilution was spotted on the agar. The plates were incubated at 37 °C for 24 h.

Activity Assay in Cell Extracts—50 ml of exponentially grown cell cultures (A_{600} = 0.2 for the culture with D-malate (0.15%) and leucine (1 mM), A_{600} = 0.1 for the culture with D-malate (0.15%), and A_{600} = 0.45 for the culture with D-glucose (0.1%) and leucine (1 mM)) were centrifuged at 4000 rpm for 10 min, and the cells were resuspended in 1 ml of KAC buffer (25 mM MOPS and 100 mM KCl, pH 7.5) (29, 42) supplemented with one tablet of Complete mini EDTA-free protease inhibitor mixture (Roche Applied Science). The samples were flash-frozen in liquid nitrogen and kept at −80 °C. For activity tests, the cells were crushed in a FastPrep-24 instrument (MP Biomedicals, Santa Ana, California) for 60 s (250 μl of glass bead suspension for 750 μl of cell suspension). The extracts were cleared by centrifugation and diluted 10 times for the activity measurements in KAC buffer. To start the reaction, 25 μl of diluted extracts was added to 125 μl of reaction mixture (500 μM D-malate or 3-isopropylmalate, 250 μM NAD^+, 5 mM $MnCl_2$, 1

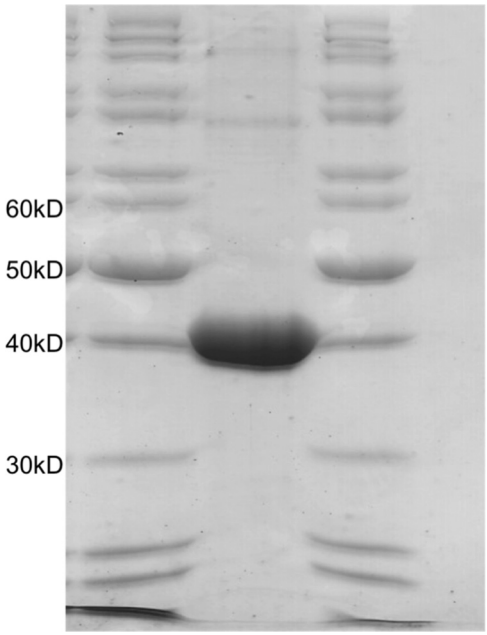

FIGURE 2. **SDS-PAGE analysis of the purified DmlA protein.** The protein was purified by *Strep*-Tactin affinity chromatography and concentrated to ~6 mg/ml (140 μM). 20 μl was loaded on the gel. The size of the DmlA monomer is 42 kDa.

mM DTT, and KAC buffer). The reaction was followed by an increase in A_{340}. The activity data were normalized to the total concentration of protein in the extracts, measured by BCA protein assay (Pierce).

DmlA Expression and Purification—The protein was expressed from BL21 cells transformed with phDmlA. Typically, 500 ml of Terrific Broth medium was inoculated and grown at 37 °C and 180 rpm until A_{600} reached 0.6. Isopropyl β-D-thiogalactopyranoside was added (1 mM final concentration), and the protein was produced at 25 °C and 180 rpm for 4 h. The cells were centrifuged and resuspended in 20 ml of buffer (100 mM Tris and 150 mM NaCl, pH 8.0) supplemented with one tablet of Complete mini EDTA-free protease inhibitor mixture and flash-frozen in liquid nitrogen. Thawed cells were treated with lysozyme (1 mg/ml, 1 h), DNase (5 μg/ml) was added for an additional 20 min, and lysis was completed by 30 min of sonication (cycles of 30 s of ultrasound and 30 s of resting on ice). The protein was purified from the cleared lysate by *Strep*-Tactin affinity chromatography (IBA, Göttingen, Germany). The fractions containing the protein were pooled, desalted (final buffer of 10 mM Tris, pH 8.0), and concentrated by ultracentrifugation in Amicon tubes (10-kDa cutoff; Millipore). The concentration of the protein was determined by measuring the absorbance at 280 nm using a predicted extinction coefficient of 64,400 M^{-1} cm^{-1} (ProtParam tool on the ExPASy server (43)). The final concentration was typically in the range of 6 mg/ml. 25-μl aliquots were flash-frozen in liquid nitrogen and kept at −80 °C. An SDS-polyacrylamide gel of the purified DmlA protein is shown in Fig. 2.

Determination of Catalytic Parameters for Different Substrates—All catalytic measurements were performed in KAC/DTT buffer (25 mM MOPS, 100 mM KCl, and 1 mM DTT, pH 7.5) at 25 °C. The pH of the substrates was adjusted to pH 7.5 with KOH. $MnCl_2$ or $MgCl_2$ (100 mM stock solutions in water) was added up to 5 mM to each reaction mixture. NAD^+ was added up to 500 μM (for D-malate and 3-isopropylmalate assays) or 2 mM (for L(+)-tartrate assays). For the other substrates, the NAD concentration was arbitrarily fixed at 1 mM to obtain apparent kinetic parameters. The reaction was started by the addition of 25 μl of the enzyme diluted in KAC/DTT buffer. The concentration of D-malate and 3-isopropylmalate ranged from 10 to 500 μM. The concentration of L(+)-tartrate ranged from 0.1 to 4 mM. tk;2Measurements were also performed with isocitrate (0.1–5 mM), D-lactate (0.1–14 mM), and D(−)-tartrate (0.1–8 mM). The fluorescence signal (340 nm excitation, 460 nm emission) was monitored over time on a Tecan Infinite 200 PRO microplate reader. Fluorescence was converted into NADH concentration using a calibration curve. The observed kinetic constants (k_{obs}) were calculated according to Equation 1,

$$k_{obs} = \frac{V_0}{[E]_0} \quad \text{(Eq. 1)}$$

where $[E]_0$ is the DmlA concentration and V_0 is the initial velocity of the reaction. Nonlinear Michaelis-Menten fitting was performed with MicroCal Origin 6.0 software (OriginLab, Northampton, MA) with Equation 2,

$$k_{obs} = \frac{k_{cat} \cdot [S]}{K_m + [S]} \quad \text{(Eq. 2)}$$

where [S] is the substrate concentration.

All measurements were performed in duplicates. The effect of pH on DmlA activity was tested by Michaelis-Menten kinetics in KAC/DTT buffer with pH adjusted to 6.0 – 8.5 (with steps of 0.5 pH unit) with HCl or KOH.

Differential Scanning Fluorometry—The protein was diluted in KAC buffer and used at a concentration of 2 μM in the unfolding assay. The substrates of the enzyme were added at a concentration of 1 mM. SYPRO Orange dye was added (5000-fold dilution of dimethyl sulfoxide stock solution, Thermo Fisher Scientific). Using an Applied Biosciences StepOnePlus RT-PCR system (Thermo Fisher Scientific), a temperature gradient of 1 °C/min (ranging from 25 to 90 °C) was applied to the samples, and dye fluorescence was monitored (emission filter at 580 nm). The unfolding data were corrected with the blank carried out under the same conditions without protein and were fitted to the Boltzmann sigmoid equation (Equation 3) describing the fluorescence intensity (y) as a function of temperature (x) (as described in Ref. 44) using MicroCal Origin 6.0 software.

$$y = LL + \frac{UL - LL}{1 + \exp\left(\frac{Tm - x}{a}\right)} \quad \text{(Eq. 3)}$$

LL and *UL* are the minimum and maximum fluorescence intensities of the transition, respectively. T_m is the melting temperature. The constant a is the slope of the curve at T_m. The measurements were done in duplicates.

Phylogenetic Analysis—We constructed a data set of ~250 homologous sequences after performing a BLAST search with *Pp*TDH as bait. The sequences were aligned, and those contain-

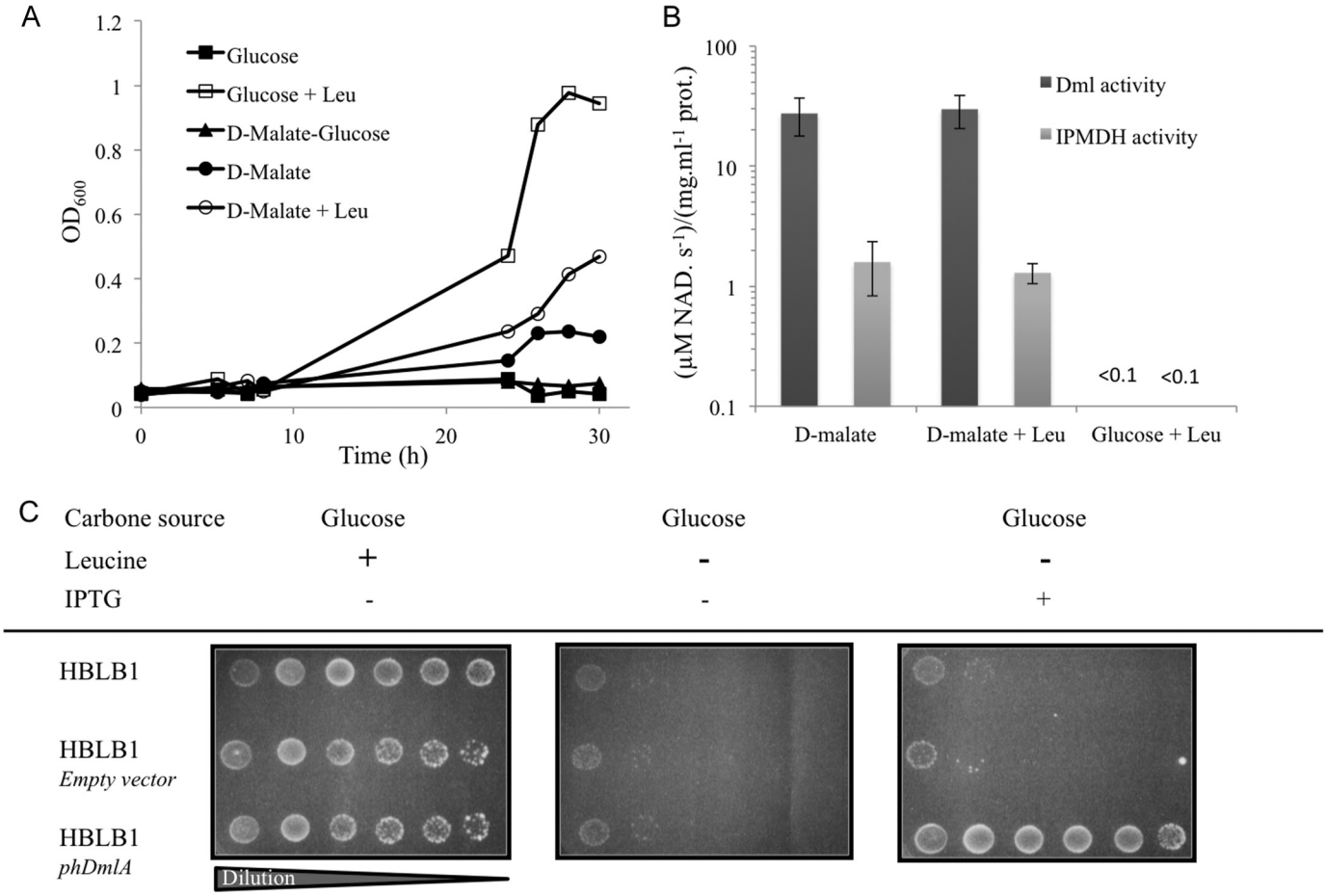

FIGURE 3. **DmlA complements the Δ*leuB* phenotype.** *A*, HBLB1 (Δ*leuB* strain) growth in liquid EZ Rich defined medium. ■, D-glucose as the carbon source (0.1%) without leucine; □, D-glucose as the carbon source (0.1%) with leucine (1 mM); ▲, D-glucose (0.1%) and D-malate (0.15%) as carbon sources; ●, D-malate as the carbon source (0.15%) without leucine; ○, D-malate as the carbon source (0.15%) with leucine (1 mM). *B*, D-malate (*dark gray bars*) and 3-isopropylmalate (*light gray bars*) dehydrogenase activities in extracts prepared from exponentially growing HBLB1 cells collected under D-malate, D-malate + leucine, and D-glucose + leucine conditions. The measured activities were normalized to the total protein concentrations. *C*, *Ec*DmlA expressed from HBLB1 cells transformed with the phDmlA vector. Complementation of leucine auxotrophy on EZ Rich defined medium depends on the presence of the isopropyl β-D-thiogalactopyranoside (*IPTG*) inducer (1 mM).

ing mutations of conserved active site residues were discarded. As most of the sequences obtained were from α-, β-, and γ-Proteobacteria, we kept only the sequences from these classes of organisms in the final data set for a more clear analysis. Sequences from fungi, archaea, and other Proteobacteria were discarded, as well as two HDH sequences. Finally, the data set was screened for highly similar sequences. We tried to keep Dml/TDHs and IPMDHs from the same organisms in the data set when it was possible. The resulting final data set contains 95 different IDH, Dml/TDH, IPMDH, and TtuC sequences (see supplemental material). The annotation attributed to some proteins did not correspond to the conserved motif in the substrate recognition structure (45). These sequences were properly re-annotated. Alignments were done with the Clustal algorithm. The best fit model for amino acid replacement was determined using the ProtTest 3 server (46). The LG +I +G model was selected. The phylogenetic tree was calculated with the PhyML program, and 100 rounds of bootstrapping analysis were performed (47). The trees were generated using the TreeDyn algorithm, available online at the Phylogeny.fr web site (48). Finally, to evaluate the robustness of the tree, similar analyses from initial Muscle and T-Coffee alignments and from the Clustal alignment using the WAG substitution model were performed. Similar conclusions could be drawn from all constructed trees.

RESULTS

*Expression of DmlA under the Control of Its Native Promoter Complements the Δ*leuB* Phenotype*—Given the high similarity of *Ec*DmlA to *Pp*TDH and the activity of *Pp*TDH detected on 3-isopropylmalate, we hypothesized that *Ec*DmlA could be responsible for suppressive *leuB* knock-out complementation. To study the IPMDH function of *Ec*DmlA *in vivo* and to avoid direct *leuB*$^{-}$ reversion, we constructed the HBLB1 strain, in which the *leuB6* gene of the HB101 strain was deleted (Δ*leuB* strain). Leucine auxotrophy was tested in chemically defined medium with different carbon sources. As shown in Fig. 3*a*, with D-glucose as the carbon source, leucine supplementation was necessary to support HBLB1 growth. With D-malate, however, HBLB1 cells grew without leucine, and growth was inhibited when glucose was added as an alternative carbon source to D-malate. The same result was obtained on solid medium (data not shown). As *Ec*DmlA expression is induced by D-malate and repressed by glucose (49), this experiment supports our initial

hypothesis. In liquid medium, A_{600} reached ~0.4 on D-malate and leucine and 0.2 on D-malate at stationary phase. The lower plateau reached by the cells in the absence of leucine indicates that the fitness of the strain is limited by either the D-malate catabolism or the synthesis of leucine, as both pathways are supported by the same enzyme and compete with each other. We collected samples of exponentially growing cells and tested the activities on D-malate (Dml) and 3-isopropylmalate (IPMDH) in the extracts. Both activities were present in cells grown on D-malate (with and without leucine) and absent from cells grown on D-glucose medium supplemented with leucine (Fig. 3*b*). No difference in the level of Dml or IPMDH activity was detected between cells grown on D-malate in the presence or absence of leucine. Altogether, these results indicate that normal induction of *Ec*DmlA by D-malate is sufficient for *leuB*$^-$ complementation and that no overexpression mechanism is involved. To confirm the role of *Ec*DmlA in leucine prototrophy, its gene was cloned in an expression plasmid under the control of the P_{tac} promoter. Competent HBLB1 cells were transformed with the resulting phDmlA vector. With glucose as the carbon source, leucine prototrophy of the phDmlA-HBLB1 strain depended on DmlA induction by isopropyl β-D-thiogalactopyranoside (IPTG) (Fig. 3*c*). Besides the selection of a few revertants, no growth was observed for the control strain transformed with the empty vector.

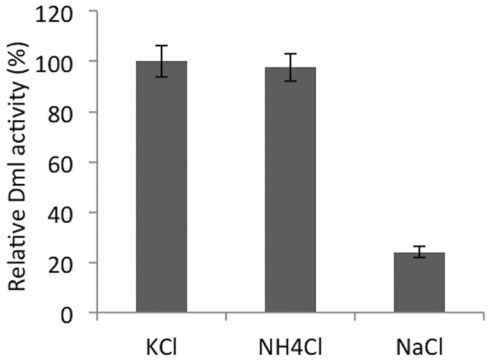

FIGURE 4. **Monovalent cations modulate the catalytic activity of DmlA.** The activity of DmlA on D-malate was tested in 25 mM MOPS buffer, pH 7.5, supplemented with 150 mM K^+, NH_4^+, or Na^+ chloride salts. The activity of the enzyme with KCl was set as the reference.

EcDmlA Is a Generalist Enzyme—*Strep*-tag II-fused *Ec*DmlA was expressed, purified, and biochemically characterized. Similar to other β-decarboxylating dehydrogenases, *Ec*DmlA activity depended on the presence of divalent metal ion (Mn^{2+} or Mg^{2+}) (data not shown). As several TDHs and HDHs are activated by K^+ or NH_4^+ and are less active in the presence of Na^+ (33, 50, 51), we tested the effect of these monovalent cations on the activity of *Ec*DmlA and found a similar behavior (Fig. 4). Enzyme kinetics (50) and structural data (27) suggest that the K^+ or NH_4^+ ion interacts with the NAD and helps in cofactor positioning. The activity-pH profile has a bell shape with an optimum at pH 7.0–7.5 (data not shown). As predicted by amino acid sequence, *Ec*DmlA preferred NAD to NADP by ~500-fold (data not shown). The activity of the enzyme on D-malate ($k_{cat}/K_{m(malate)} = 10^5\ M^{-1}\ s^{-1}$) (Table 1) corresponded to that reported for a moderately efficient enzyme in energy metabolism (52). Strikingly, the enzyme exhibited high activity on 3-isopropylmalate, with $k_{cat}/K_{m(IPM)} = 4 \times 10^3\ M^{-1}\ s^{-1}$. This is only 50 times lower than the constant for *Ec*IPMDH at the same temperature ($k_{cat}/K_{m(IPM)} = 2 \times 10^5\ M^{-1}\ s^{-1}$) (28), supporting *leuB*$^-$ complementation. Finally, significant activity on L(+)-tartrate was also detected ($k_{cat}/K_{m(L\text{-}(+)\text{-}tartrate)} = 5 \times 10^2\ M^{-1}\ s^{-1}$). The impact of divalent metal ion on substrate specificity was investigated by replacing Mn^{2+} with Mg^{2+} for activity measurements. With the Mg^{2+} metal ion, all three activities decreased by 2–5-fold, but their relative levels remained roughly unchanged (data not shown).

The k_{cat}/K_m parameters obtained for *Ec*DmlA are very similar to the data reported for *Pp*TDH at the same temperature for D-malate, 3-isopropylmalate, and L(+)-tartrate (Table 1; data from Ref. 33). However, overexpressed *Ec*DmlA did not afford any growth of the HBLB1 strain on L(+)-tartrate in the presence of 1 mM leucine (data not shown). In a similar experiment, Lukas *et al.* (49) reported a very slow growth but only when the medium was enriched with amino acids. The turnover rate constant (k_{cat}) of DmlA with L(+)-tartrate was twice as high as that with 3-isopropylmalate. However, the K_m for L(+)-tartrate and

TABLE 1

Apparent kinetic parameters determined for *Ec*DmlA on different substrates and in the presence of different divalent metal ions

The concentration of Mn^{2+} was fixed at 5 mM for all measurements. The measurements were done at 25 °C and pH 7.5 in the presence of 150 mM KCl. The rate *versus* substrate concentration data are presented in Fig. 6. ND, not determined.

	*Ec*DmlA					*Pp*TDH[c]
	k_{cat}	$K_{m(substrate)}$[a]	$k_{cat}/K_{m(substrate)}$	$K_{m(NAD)}$[b]	$k_{cat}/K_{m(NAD)}$	$k_{cat}/K_{m(substrate)}$
	s^{-1}	μM	$M^{-1}\ s^{-1}$	μM	$M^{-1}\ s^{-1}$	$M^{-1}\ s^{-1}$
D-Malate[d]	11.7 ± 0.3	96 ± 7	1×10^5	94 ± 8	1×10^5	2×10^5
3-Isopropylmalate[d]	0.102 ± 0.003	24 ± 3	4×10^3	70 ± 3	2×10^3	1×10^4
L(+)-Tartrate[d]	0.26 ± 0.01	567 ± 84	5×10^2	600 ± 200	5×10^2	4×10^2
D-Isocitrate[f]	(5.4 ± 0.2) × 10^{-4}	1300 ± 125	4×10^{-1}	ND	ND	ND
D(−)-Tartrate[f,g]	ND	≥8000	3×10^{-1}	ND	ND	ND
D-Lactate[f,g]	ND	≥14,000	1×10^{-1}	ND	ND	ND

[a] Apparent K_m for the specified substrate with a fixed concentration of NAD.
[b] Apparent K_m for NAD with a fixed concentration of the specified substrate.
[c] Data are taken from Ref. 33.
[d] For these substrate, the concentration of NAD was fixed at 500 μM for the $K_{m(substrate)}$ measurements, and the concentration of substrates was fixed at 500 μM for the $K_{m(NAD)}$ measurements.
[e] For L(+)-tartrate, the concentration of NAD was fixed at 2 mM for the $K_{m(substrate)}$ measurements, and the concentration of substrates was fixed at 5 mM for the $K_{m(NAD)}$ measurements.
[f] For these substrates, the concentration of NAD was fixed at 1 mM to obtain apparent $k_{cat}/K_{m(substrate)}$.
[g] Because of the high $K_{m(substrate)}$, the kinetic parameters could not be obtained for these substrates, and the $k_{cat}/K_{m(substrate)}$ values were estimated from the linear part of the Michaelis-Menten function.

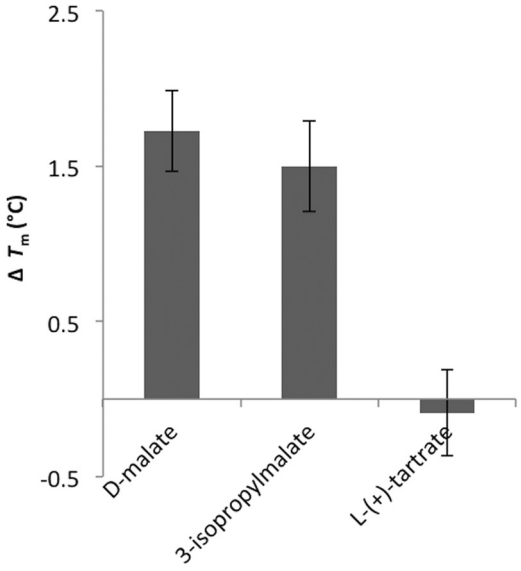

FIGURE 5. **DmlA unfolds at a higher temperature in the presence of D-malate and 3-isopropylmalate, but not L-(+)-tartrate.** T_m was measured by differential scanning fluorometry of the apo form and in the presence of 1 mM D-malate, 3-isopropylmalate, and L(+)-tartrate. The ΔT_m values represent the difference in T_m between the protein in the presence of the specified substrate and the apoprotein.

NAD was 5–20-fold higher than the K_m for all previously tested substrates. Additionally, a low affinity of *Ec*DmlA for L(+)-tartrate was suggested by thermal unfolding of the protein in a differential scanning fluorometry experiment (Fig. 5). In a differential scanning fluorometry assay, the temperature at which a protein unfolds in the presence of a ligand is compared with its unfolding temperature in the apo form. The stabilizing effect increases with binding affinity (53, 54). In the presence of 1 mM D-malate or 3-isopropylmalate, the protein unfolded at higher temperature compared with its apo form (1.5–2 °C higher T_m). In contrast, no significant T_m shift was observed in the presence of the same concentration of L(+)-tartrate, indicating that the interaction between *Ec*DmlA and L(+)-tartrate is weaker than the interaction between *Ec*DmlA and D-malate or 3-isopropylmalate. Notably, L(+)-tartrate is the only substrate in Fig. 1 with C-3 in the *R*-configuration, whereas all other substrates feature the *S*-configuration. The increase in K_m for both L(+)-tartrate and NAD may be explained by steric hindrance between the substrate and cofactor or between the substituent on C-3 of L(+)-tartrate and a structural part of the active site.

In the results presented above, we showed that *Ec*DmlA was active on a substrate with a large hydrophobic γ-substituent (3-isopropylmalate), as well as a substrate with hydrogen in that position (D-malate) and a substrate with a polar hydroxyl as a γ-substituent in an inverted configuration (L(+)-tartrate). We further observed a weak activity of the enzyme on isocitrate ($k_{cat}/K_{m(\text{isocitrate})} = 4 \times 10^{-1}\ \text{M}^{-1}\ \text{s}^{-1}$), a molecule with a negatively charged γ-substituent. D-Lactate, a minimalist substrate without the C-4 carboxyl, was also a poor substrate for *Ec*DmlA ($k_{cat}/K_{m(\text{lactate})} = 1 \times 10^{-1}\ \text{M}^{-1}\ \text{s}^{-1}$). Finally, the enzyme was also active on D(−)-tartrate ($k_{cat}/K_{m(\text{D-(−)-tartrate})} = 3 \times 10^{-1}\ \text{M}^{-1}\ \text{s}^{-1}$), which has C-3 in the preferred *S*-configuration but features an inverted configuration of C-2 involved in hydride transfer with the cofactor. Hence, *Ec*DmlA is a highly versatile enzyme and accepts substrates featuring different sizes and polarities of the γ-substituent, a carboxyl or a hydrogen as the other substituent of C-3, and both configurations of C-2 and C-3. The rate *versus* substrate concentration data for all tested substrates are shown in Fig. 6.

Phylogenetic Analysis Suggests an Ancient Origin for Dml/TDH Enzymes—D-Malate/tartrate dehydrogenases are metabolic enzymes supporting aerobic growth either on D-malate (Dml activity) or on L(+)-tartrate (TDH and TtuC activities). It is important to emphasize that the current data on the Dml/TDH family are limited, especially at the metabolic level. Hence, the enzymes hereafter are annotated according to their initial characterization (Dml or TDH), which may not precisely reflect their actual metabolic role(s). So far, biochemical data are available for *Pp*TDH, *Pseudomonas fluorescens* TDH (55), and *Rhodobacter sphaeroides* TDH (51), as well as *Ec*DmlA (this study). Additionally, the metabolic role of two other proteins was experimentally confirmed: D-malate growth for *Enterobacter aerogenes* Dml (55) and L(+)-tartrate growth for *Agrobacterium vitis* TtuC (56).

The phylogenetic analysis of a data set of sequences homologous to *Pp*TDH and *Ec*DmlA (minimum 35% identity) showed that the sequences cluster into three groups: the IPMDHs, NAD-dependent IDHs, and Dml/TDHs (Fig. 7). In the data set, the function of the proteins was assigned using the conserved motifs in the substrate recognition region identified by Chen and Jeong (45). The motif S*X*N is conserved in IDHs, whereas the motifs EX_{2-3}(L/I)L and LX_3L are proper to 3-isopropylmalate and D-malate/tartrate dehydrogenases, respectively (45, 57).

The evolutionary trajectory that was hypothesized for explaining the low activity of *Pp*TDH on L(+)-tartrate and its activity on isopropylmalate starts by a recent duplication of an IPMDH gene, followed by the evolution of the enzyme into a generalist, and ends with the partial re-specialization for the new catalytic function (33). However, the topology of our phylogenetic tree suggests that the Dml/TDH activity is more ancient than previously thought. Instead of branching to the IPMDH cluster, the Dml/TDHs are monophyletic and diverge more or less from the same point as the NAD-dependent IDHs and IPMDHs. Hence, Dml/TDH proteins likely evolved directly from the common ancestor of the β-decarboxylating dehydrogenases that was proposed to be a generalist enzyme (58) rather than from a duplicated IPMDH gene. Another interesting observation is that the generalist character seems to be a common feature of the Dml/TDH enzymes. Activity on D-malate, L(+)-tartrate, and 3-isopropylmalate was reported for *Pp*TDH and *Ec*DmlA, sharing 76% identity along the entire sequence length. D-Malate and tartrate activities were also reported for *R. sphaeroides* TDH, sharing 60 and 65% identities, respectively, with the two others and located in a different phylogenetic subcluster. The highest activity of the purified *R. sphaeroides* TDH, the Dml activity, is only 2 orders of magnitude higher than its TDH activity (in terms of k_{cat}/K_m) (51). Moreover, *R. sphaeroides* TDH supports the growth of *R. sphaeroides* on L(+)-tartrate. The activity of this enzyme toward 3-isopropylmalate was not tested. The promiscuous properties of these three divergent enzymes suggest that the generalist trait was maintained through the evolution of Dml/TDHs.

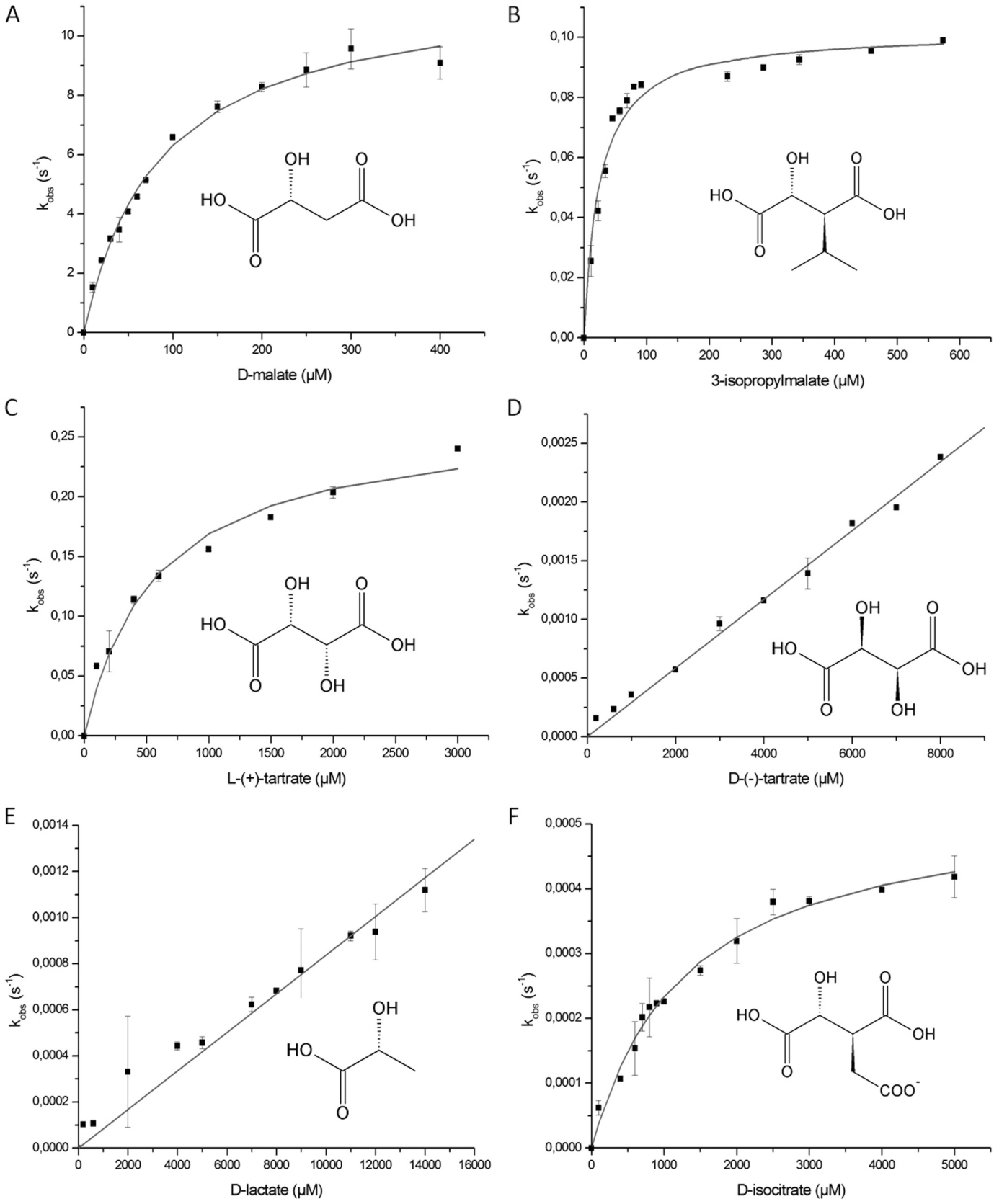

FIGURE 6. **Kinetic characterization of DmlA on various substrates.** The k_{obs} values were measured for six substrates at different concentrations with fixed concentrations of NAD^+ (see "Experimental Procedures" for concentrations) and Mn^{2+} (5 mM). The kinetic parameters were calculated from the data by fitting to the Michaelis-Menten equation (Equation 2) (*A–C* and *F*) and by estimating the k_{cat}/K_m parameter from the linear part of the activity-substrate curve (*D* and *E*). The calculated parameters are reported in Table 1.

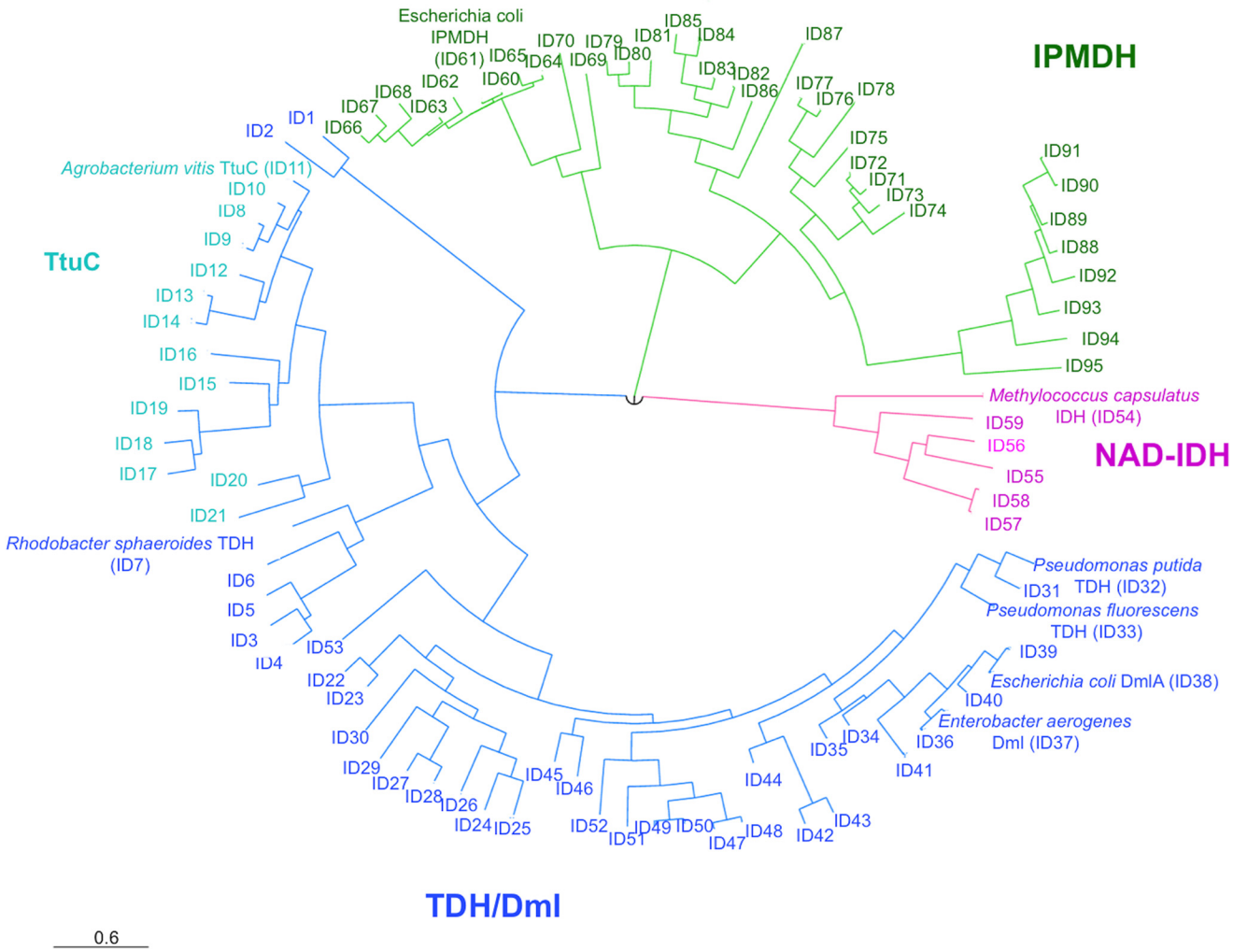

FIGURE 7. **Phylogenetic relationship between Dml/TDHs, IPMDHs, and IDHs.** The unrooted phylogenetic tree shows the evolutionary relationship between IPMDHs (*green*), NAD-dependent IDHs (*pink*), and Dml/TDH/TtuC enzymes (Dml/TDHs are *blue*, and TtuC enzymes are *cyan*) from α-, β-, and γ-Proteobacteria. The protein names are indicated for those proteins that have been characterized *in vivo* and/or *in vitro* (28, 51, 55, 56, 66). The other proteins are designed with an ID number referring to the complete data set presented in the supplemental material.

The phylogenetic tree also shows that TtuC-like proteins form a subcluster among the D-malate/tartrate dehydrogenases (Fig. 7). Surprisingly, some active site residues that are usually conserved in the enzymes of the β-decarboxylating dehydrogenase superfamily are modified in TtuC proteins (Table 2). First, the last leucine of the L*XXX*L motif specific to the substrate recognition loop of the Dml/TDH enzymes is replaced with arginine. Second, Arg-97 (*Ec*DmlA numbering), which is conserved in all β-decarboxylating dehydrogenases and interacts with both carboxylates of the common D-malate moiety of the substrates, is mutated to cysteine in TtuC proteins. Despite these mutations, *A. vitis* TtuC is essential for growth on L(+)-tartrate (56). This suggests a unique substrate-binding mechanism among the β-decarboxylating dehydrogenases. As many organisms, such as *R. sphaeroides*, *Klebsiella pneumoniae*, and *Agrobacterium tumefaciens*, contain both TtuC and TDH, the enzymes may have different metabolic roles or functions.

DISCUSSION

In this work, we have shown that the promiscuous activity of wild-type and naturally expressed *Ec*DmlA on 3-isopropylmalate is high enough to complement the knock-out of the paralogous LeuB enzyme from the leucine biosynthesis pathway. Moreover, *Ec*DmlA is simultaneously active in its original D-malate catabolism pathway and in the leucine biosynthesis pathway. The bifunctionality is significant because relatively high fluxes through these two pathways are essential to the bacteria under the applied growth conditions. To our knowledge, this result provides the first experimental example of a wild-type generalist enzyme supporting two core metabolic fluxes *in vivo* in the absence of protein overexpression. The capacity of *Ec*DmlA to function in both metabolic pathways is explained by its high catalytic activity on D-malate and isopropylmalate. The enzyme also has a relatively high activity on L(+)-tartrate, although our results indicate a weak affinity of the protein for this alternative substrate compared with D-malate and 3-isopropylmalate. This can be linked to the work on *Pp*TDH done by Serfozo and Tipton (59, 60), who suggested a common binding mode for substrates featuring the *S*-configuration of C-3 (D-malate, 3-isopropylmalate) and an alternative binding mode for substrates featuring the *R*-configuration of C-3 (L(+)-tartrate). The alternative *R*-configuration binding

TABLE 2

Alignment of several IPMDH, Dml/TDH, TtuC, and NAD-dependent IDH proteins in the substrate recognition region

The numbers indicate the amino acid numbering of the first sequence from each group of enzymes. The conserved residues, identified as conserved motifs, are shown in boldface. The complete set of sequences used for the phylogenetic analysis and the alignment of the substrate recognition regions is provided in the supplemental material.

IPMDH	90	91	92	93	94	95	96	97	98	99	100
E. coli	P	**E**	R	G	A	**L**	**L**	P	L	**R**	K
Pseudomonas putida	P	**E**	R	G	-	**L**	**L**	K	I	**R**	S
Bordetella holmesii	P	**E**	Q	A	-	**I**	**L**	G	L	**R**	K
Dml/TDH	88	89	90	91	92	93	94	95	96	97	98
E. coli	S	**L**	W	G	S	**L**	L	K	F	**R**	R
Acinetobacter baumannii	S	**L**	W	G	S	**L**	L	Q	F	**R**	R
Rhodobacter sphaeroides	S	**L**	H	G	L	**L**	L	P	I	**R**	K
TtuC	88	89	90	91	92	93	94	95	96	97	98
Rhodobacter sphaeroides	T	**L**	W	G	L	**R**	L	A	I	**C**	Q
Klebsiella pneumoniae	T	**L**	W	G	L	**R**	L	P	I	**C**	Q
Agrobacterium vitis	T	**L**	W	G	L	**R**	L	P	I	**C**	Q
NAD-IDH	99	100	101	102	103	104	105	106	107	108	109
Halomonas boliviensis	G	F	S	**S**	I	**N**	V	Q	L	**R**	R
Methylococcus capsulatus	G	F	S	**S**	I	**N**	V	Q	L	**R**	R

mode has not been characterized yet and was proposed to explain the release of the oxidized intermediate without further decarboxylation. As the kinetic values obtained for *Ec*DmlA are very similar to the kinetic values reported for *Pp*TDH on all three substrates (33), the catalytic mechanisms of both enzymes should be similar, and the inability of *Ec*DmlA overexpression to support growth of the bacteria on L(+)-tartrate is more likely due to a lack of membrane transporters for L(+)-tartrate or to metabolic differences between *E. coli* and *P. putida*.

Enzymes are generally described in textbooks as remarkable specialists. However, the number of promiscuous enzymes reported in the literature is rapidly growing, suggesting that most enzymes promiscuously accept alternative substrates (13). *Ec*DmlA is a remarkable example because it features relatively high activities on three different substrates and may therefore be defined as a generalist. Moreover, the topology of our phylogenetic tree suggests that Dml/TDHs are ancient and emerged about the time when the core metabolic pathways of leucine biosynthesis and the Krebs cycle diverged. Because the three Dml/TDHs that have been biochemically characterized accept multiple substrates and are well dispersed in the tree, the whole family most probably shares the generalist trait, although a more systematic study would be necessary to confirm this hypothesis.

Why was *Ec*DmlA maintained as a generalist in the course of evolution? Was it selected for several activities, or is it just the result of fortuitous enzyme infidelity (*i.e.* promiscuity (61))? The later hypothesis is supported by the regulation mechanism of the *dmlA* gene. The expression of the protein is determined by the carbon source used, independent of the presence or absence of leucine, because no overexpression could be detected under leucine starvation conditions. This indicates that its IPMDH activity is a consequence of enzyme infidelity rather than a selected alternative route for leucine biosynthesis. We propose two hypotheses to explain the evolutionary retention of the generalist trait.

(i) The selection pressure for specialization may be low. In other words, promiscuity may be maintained as long as it does not interfere with any metabolic function. Although *Ec*DmlA will have to support a high metabolic flux when D-malate is used as the carbon source, these conditions may be very occasional (49). Moreover, when DmlA is expressed in a wild-type strain with an active leucine biosynthesis pathway, the two pathways will probably not interfere significantly. Indeed, as an intermediate metabolite, 3-isopropylmalate will probably be maintained at a low concentration. In contrast, if a source of exogenous leucine is present in the medium, the expression of the genes encoded in the *leu* operon will be down-regulated (62), and the intracellular concentration of the intermediate metabolites will be even lower.

(ii) The full specialization may be difficult to achieve in this particular active site scaffold. Indeed, the positioning of the cofactor relative to the substrate is a critical aspect for catalysis by the β-decarboxylating dehydrogenases (63, 64). The cofactor may be constrained to its optimal conformation by active site residues (as for IPMDHs (63)) or by the γ-substituent of the substrate (as for IDHs (64)). For *Pp*TDH, structural data suggest that cofactor positioning probably involves an interaction with the monovalent cation (K^+ or NH_4^+) that is necessary for catalysis (27, 33). However, the interactions between K^+ ions and their ligands are dominantly electrostatic, and a wider range of distances and coordination numbers are then acceptable (65). An active site geometry shaped by a K^+ ion would probably allow more conformational changes to accommodate different substrates. This hypothesis is supported by the biochemical data obtained for other β-decarboxylating dehydrogenases. Indeed, among the biochemically characterized HDHs, the cation-dependent HDH of *D. radiodurans* features broader substrate specificity than the HDHs of *T. thermophilus* and *P. horikoshii*, which do not require any monovalent cation (30–32). The IDHs and IPMDHs, which are cation-independent, are more specific to their respective natural substrates.

How can the generalist traits of an enzyme impact the metabolic plasticity of the organism? Enzyme promiscuous activities are believed to be good starting points for evolution by providing possibilities of innovation before or after a gene duplication event. As discussed in the Introduction, McLoughlin and Copley (15) reported an example of an enzyme featuring one unique mutation that affords bifunctionality but at the expense of a significant negative trade-off between the new and old functions. Hence, at the early stage of evolution, a compromise between the newly evolved and original activities has to be found to allow the survival of the organism. The particular example of *Ec*DmlA shows that a secondary high level activity may coexist with the original one without any mutation-associated compromise. Despite the fact that the activity of the enzyme on 3-isopropylmalate is high ($k_{cat}/K_m \sim 10^3\ M^{-1}\ s^{-1}$) and sufficient to affect the phenotype of the organism, its principal activity on D-malate remains compatible with an efficient enzyme from secondary metabolism (52). There is, however, a compromise imposed by gene sharing but at the metabolic level when both activities are simultaneously required. Indeed, the

growth of the Δ*leuB* strain on D-malate is lower when exogenous leucine is absent, indicating a competition between the two metabolic pathways sustained by the same enzyme. If the selection pressure for one or both activities increases because higher or more constant metabolic fluxes are required, the fitness will probably improve upon a simple overexpression of the protein by mutation in the promoter region or by gene duplication. Interestingly, sequence alignments suggest that TtuC enzymes form a distinct cluster among Dml/TDHs and feature a different substrate-binding motif. The gene coding for TtuC of *A. vitis* (a grapevine pathogen) belongs to the tartrate operon (*ttu*), suggesting that TtuC-like enzymes could have arisen from the specialization of a *tdh* gene for tartrate utilization (56). In *A. tumefaciens*, the *ttuC* gene is encoded in a similar tartrate *ttu* operon and coexists with a *tdh* gene (see supplemental material), suggesting a gene duplication scenario. If TtuC enzymes evolved to efficiently catabolize tartrate, then this specialization required consequent mutations of otherwise conserved residues. Hence, a deeper study of substrate specificities among Dml/TDHs regarding the potential existence of structural features promoting enzyme promiscuity or specialization and the trade-offs between the different activities in the course of evolution would be very informative.

Are these results relevant in the context of natural evolution? The experimental design applied in this study is artificial, as a metabolic limitation was created by the knock-out of a metabolically important gene. However, it mimics a new requirement for neofunctionalization that could arise naturally due to environmental changes. It is yet unclear if other proteins have secondary activities close to a physiologically relevant level. In particular, it is important to emphasize that all of the systematic screenings for enzyme generalists were realized under overexpression conditions using multicopy vectors (9, 10). However, some of the enzymes selected in these studies may be sufficiently active on the alternative substrates to afford a phenotype without overexpression. Previous studies (11, 15) showed that a single mutation in a chromosomal gene might increase a promiscuous activity at a level sufficient to complement a metabolic knock-out. Hence, the development of new techniques for directed evolution of chromosome-encoded proteins is a key challenge for gaining further insight into the mechanisms governing natural evolution of enzymes.

Acknowledgments—We acknowledge Prof. Jean-François Collet (Université catholique de Louvain) for providing the strain from the Keio Collection. We also thank Dr. Florian Hollfelder (University of Cambridge, Cambridge, United Kingdom) for comments on the manuscript.

REFERENCES

1. Ohno, S. (1970) *Evolution by Gene Duplication*, Springer-Verlag, New York.
2. Voordeckers, K., Brown, C. A., Vanneste, K., van der Zande, E., Voet, A., Maere, S., and Verstrepen, K. J. (December 11, 2012) Reconstitution of ancestral metabolic enzymes reveals molecular mechanisms underlying evolutionary innovation through gene duplication. *PloS Biol.* **10,** e1001446
3. Huang, R., Hippauf, F., Rohrbeck, D., Haustein, M., Wenke, K., Feike, J., Sorrelle, N., Piechulla, B., and Barkman, T. J. (2012) Enzyme functional evolution through improved catalysis of ancestrally nonpreferred substrates. *Proc. Natl. Acad. Sci. U.S.A.* **109,** 2966–2971
4. Jensen, R. A. (1976) Enzyme recruitment in evolution of new function. *Annu. Rev. Microbiol.* **30,** 409–425
5. Copley, S. D. (2012) Toward a systems biology perspective on enzyme evolution. *J. Biol. Chem.* **287,** 3–10
6. Glasner, M. E., Gerlt, J. A., and Babbitt, P. C. (2006) Evolution of enzyme superfamilies. *Curr. Opin. Chem. Biol.* **10,** 492–497
7. Afriat, L., Roodveldt, C., Manco, G., and Tawfik, D. S. (2006) The latent promiscuity of newly identified microbial lactonases is linked to a recently diverged phosphotriesterase. *Biochemistry* **45,** 13677–13686
8. van Loo, B., Jonas, S., Babtie, A. C., Benjdia, A., Berteau, O., Hyvönen, M., and Hollfelder, F. (2010) An efficient, multiply promiscuous hydrolase in the alkaline phosphatase superfamily. *Proc. Natl. Acad. Sci. U.S.A.* **107,** 2740–2745
9. Patrick, W. M., Quandt, E. M., Swartzlander, D. B., and Matsumura, I. (2007) Multicopy suppression underpins metabolic evolvability. *Mol. Biol. Evol.* **24,** 2716–2722
10. Soo, V. W., Hanson-Manful, P., and Patrick, W. M. (2011) Artificial gene amplification reveals an abundance of promiscuous resistance determinants in *E. coli*. *Proc. Natl. Acad. Sci. U.S.A.* **108,** 1484–1489
11. Yip, S. H., and Matsumura, I. (2013) Substrate ambiguous enzymes within the *E. coli* proteome offer different evolutionary solutions to the same problem. *Mol. Biol. Evol.* **30,** 2001–2012
12. Khersonsky, O., Roodveldt, C., and Tawfik, D. S. (2006) Enzyme promiscuity: evolutionary and mechanistic aspects. *Curr. Opin. Chem. Biol.* **10,** 498–508
13. Khersonsky, O., and Tawfik, D. S. (2010) Enzyme promiscuity: a mechanistic and evolutionary perspective. *Annu. Rev. Biochem.* **79,** 471–505
14. Kaltenbach, M., and Tokuriki, N. (2014) Dynamics and constraints of enzyme evolution. *J. Exp. Zool. B Mol. Dev. Evol.* **9999,** 1–20
15. McLoughlin, S. Y., and Copley, S. D. (2008) A compromise required by gene sharing enables survival: implications for evolution of new enzyme activities. *Proc. Natl. Acad. Sci. U.S.A.* **105,** 13497–13502
16. Miller, B. G., and Raines, R. T. (2004) Identifying latent enzymes activities: substrate ambiguity within modern bacteria sugar kinases. *Biochemistry* **43,** 6387–6392
17. Miller, B. G., and Raines, R. T. (2005) Reconstitution of a defunct glycolytic pathway via recruitment of ambiguous sugar kinases. *Biochemistry* **44,** 10776–10783
18. Yang, K., and Metcalf, W. W. (2004) A new activity for an older enzyme: *Escherichia coli* bacterial alkaline phosphatase is a phosphite-dependent dehydrogenase. *Proc. Natl. Acad. Sci. U.S.A.* **101,** 7919–7924
19. Nam, H., Lewis, N. E., Lerman, J. A., Lee, D. H., Chang, R. L., Kim, D., and Palsson, B. O. (2012) Network context and selection in the evolution to enzyme specificity. *Science* **337,** 1101–1104
20. D'Ari, R., and Casadesús, J. (1998) Underground metabolism. *BioEssays* **20,** 181–186
21. Fedøy, A. E., Yang, N., Martinez, A., Leiros, H. K., and Steen, I. H. (2007) Structural and functional properties of isocitrate dehydrogenase from the psychrophilic bacterium *Desulfotalea psychrophila* reveal a cold-active enzyme with an unusual high thermal stability. *J. Mol. Biol.* **371,** 130–149
22. Hurley, J. H., Thorsness, P. E., Ramalingam, V., Helmers, N. H., Koshland, D. E., Jr., and Stroud R. M. (1989) Structure of a bacterial enzyme regulated by phosphorylation, isocitrate dehydrogenase. *Proc. Natl. Acad. Sci. U.S.A.* **86,** 8635–8639
23. Stokke, R., Karlström, M., Yang, N., Leiros, I., Ladenstein, R., Birkeland, N. K., and Steen, I. H. (2007) Thermal stability of isocitrate dehydrogenase from *Archaeoglobus fulgidus* studied by crystal structure analysis and engineering of chimers. *Extremophiles* **11,** 481–493
24. Gráczer, É., Merli, A., Singh, R. K., Karuppasamy, M., Závodszky, P., Weiss, M. S., and Vas, M. (2011) Atomic level description of the domain closure in a dimeric enzyme: *Thermus thermophilus* 3-isopropylmalate dehydrogenase. *Mol. Biosyst.* **7,** 1646–1659
25. Wallon, G., Kryger, G., Lovett, S. T., Oshima, T., Ringe, D., and Petsko, G. A. (1997) Crystal structure of *E. coli* and *Salmonella typhimurium* 3-isopropylmalate dehydrogenase and comparison with their thermophilic counterpart from *Thermus thermophilus*. *J. Mol. Biol.* **266,** 1016–1031
26. Miyazaki, J., Asada, K., Fushinobu, S., Kuzuyama, T., and Nishiyama, M. (2005) Crystal structure of the tetrameric homoisocitrate dehydrogenase from an extreme thermophile, *Thermus thermophilus*: involvement of hydrophobic dimer-dimer interaction in extremely high thermotolerance. *J. Bacteriol.* **187,** 6779–6788

27. Malik, R., and Viola, R. E. (2010) Structural characterization of tartrate dehydrogenase: a versatile enzyme catalyzing multiple reactions. *Acta Crystallogr. D Biol. Crystallogr.* **66,** 673–684
28. Miyazaki, K., Kakinuma, K., Terasawa, H., and Oshima, T. (1993) Kinetic analysis on the substrate specificity of 3-isopropylmalate dehydrogenase. *FEBS Lett.* **332,** 35–36
29. Dean, A. M., Shiau, A. K., and Koshland, D. E., Jr. (1996) Determinants of performance in the isocitrate dehydrogenase of *Escherichia coli*. *Protein Sci.* **5,** 341–347
30. Miyazaki, K. (2005) Identification of a novel trifunctional homoisocitrate dehydrogenase and modulation of the broad substrate specificity through site-directed mutagenesis. *Biochem. Biophys. Res. Commun.* **336,** 596–602
31. Miyazaki, J., Kobashi, N., Nishiyama, M., and Yamane, H. (2003) Characterization of homoisocitrate dehydrogenase involved in lysine biosynthesis of an extremely thermophilic bacterium, *Thermus thermophilus* HB27, and evolutionary implication of β-decarboxylating dehydrogenase. *J. Biol. Chem.* **278,** 1864–1871
32. Miyazaki, K. (2005) Bifunctional isocitrate-homoisocitrate dehydrogenase: a missing link in the evolution of β-decarboxylating dehydrogenase. *Biochem. Biophys. Res. Commun.* **331,** 341–346
33. Tipton, P. A., and Beecher, B. S. (1994) Tartrate dehydrogenase, a new member of the family of metal-dependent decarboxylating *R*-hydroxyacid dehydrogenases. *Arch. Biochem. Biophys.* **313,** 15–21
34. Tipton, P. A., and Peisach, J. (1990) Characterization of the multiple catalytic activities of tartrate dehydrogenase. *Biochemistry* **29,** 1749–1756
35. Stern, J. R., and Hegre C. S. (1966) Inducible D-malic enzyme in *E. coli*. *Nature* **212,** 1611–1612
36. Reed, J. L., Patel, T. R., Chen, K. H., Joyce, A. R., Applebee, M. K., Herring, C. D., Bui, O. T., Knight, E. M., Fong, S. S., and Palsson, B. O. (2006) Systems approach to refining genome annotation. *Proc. Natl. Acad. Sci. U.S.A.* **103,** 17480–17484
37. Wright, B. E., and Minnick, M. F. (1997) Reversion rates in a *leuB* auxotroph of *E. coli* K-12 correlate with ppGpp levels during exponential growth. *Microbiology* **143,** 847–854
38. Jin, J., Gao, P., and Mao, Y. (2002) Occurence of *leu*$^+$ revertants under starvation cultures in *E. coli* is growth-dependent. *BMC Genet.* **3,** 6
39. Thomason, L. C., Costantino, N., and Court, D. L. (2007) *E. coli* genome manipulation by P1 transduction. *Curr. Protoc. Mol. Biol.* **79,** 1.17.1–1.17.8
40. Baba, T., Ara, T., Hasegawa, M., Takai, Y., Okumura, Y., Baba, M., Datsenko, K. A., Tomita, M., Wanner, B. L., and Mori, H. (February 21, 2006) Construction of *E. coli* K-12 in-frame, single-gene knockout mutants: the Keio collection. *Mol. Syst. Biol.* **2,** 2006.0008
41. Neidhardt, F. C., Bloch, P. L., and Smith, D. F. (1974) Culture medium for enterobacteria. *J. Bacteriol.* **119,** 736–747
42. Dean, A. M., Lee, M. H., and Koshland, D. E., Jr. (1989) Phosphorylation inactivates *E. coli* isocitrate dehydrogenase by preventing isocitrate binding. *J. Biol. Chem.* **264,** 20482–20486
43. Gasteiger, E., Hoogland, C., Gattiker, A., Duvaud, S., Wilkins, M. R., Appel, R. D., and Bairoch, A. (2005) Protein identification and analysis tools on the ExPASy server. in *The Proteomics Protocols Handbook* (Walker, J. M., ed), pp. 571–607, Humana Press, Totowa, NJ
44. Niesen, F. H., Berglund, H., and Vedadi, M. (2007) The use of differential scanning fluorimetry to detect ligand interactions that promote protein stability. *Nat. Protoc.* **2,** 2212–2221
45. Chen, R., and Jeong, S. S. (2000) Functional prediction: identification of protein orthologs and paralogs. *Protein Sci.* **9,** 2344–2353
46. Darriba, D., Taboada, G. L., Doallo, R., and Posada, D. (2011) ProtTest 3: fast selection of best-fit models of protein evolution. *Bioinformatics* **27,** 1164–1165
47. Guindon, S., Dufayard, J. F., Lefort, V., Anisimova, M., Hordijk, W., and Gascuel, O. (2010) New algorithms and methods to estimate maximum-likelihood phylogenies: assessing the performance of PhyML 3.0. *Syst. Biol.* **59,** 307–321
48. Dereeper, A., Guignon, V., Blanc, G., Audic, S., Buffet, S., Chevenet, F., Dufayard, J. F., Guindon, S., Lefort, V., Lescot, M., Claverie, J. M., and Gascuel, O. (2008) Phylogeny.fr: robust phylogenetic analysis for the non-specialist. *Nucleic Acids Res.* **36,** W465–W469
49. Lukas, H., Reimann, J., Kim, O. B., Grimpo, J., and Unden, G. (2010) Regulation of aerobic and anaerobic D-malate metabolism of *E. coli* by the LysR-type regulator DmlR (YeaT). *J. Bacteriol.* **192,** 2503–2511
50. Lin, Y., West, A. H., and Cook, P. F. (2008) Potassium is an activator of homoisocitrate dehydrogenase from *Saccharomyces cerevisiae*. *Biochemistry* **47,** 10809–10815
51. Giffhorn, F., and Kuhn, A. (1983) Purification and characterization of a bifunctional L-(+)-tartrate dehydrogenase-D-(+)-malate dehydrogenase (decarboxylating) from *Rhodopseudomonas sphaeroides* Y. *J. Bacteriol.* **155,** 281–290
52. Bar-Even, A., Noor, E., Savir, Y., Liebermeister, W., Davidi, D., Tawfik, D. S., and Milo, R. (2011) The moderately efficient enzyme: evolutionary and physicochemical trends shaping enzyme parameters. *Biochemistry* **50,** 4402–4410
53. Matulis, D., Kranz, J. K., Salemme, F. R., and Todd, M. J. (2005) Thermodynamic stability of carbonic anhydrase: measurements of binding affinity and stoichiometry using ThermoFluor. *Biochemistry* **44,** 5258–5266
54. Senisterra, G. A., Markin, E., Yamazaki, K., Hui, R., Vedadi, M., and Awrey, D. E. (2006) Screening for ligands using a generic and high-throughput light-scattering-based assay. *J. Biomol. Screen.* **11,** 940–948
55. Knichel, W., and Radler, F. (1982) D-Malic enzyme of *Pseudomonas fluorescens*. *Eur. J. Biochem.* **123,** 547–552
56. Crouzet, P., and Otten, L. (1995) Sequence and mutational analysis of a tartrate utilization operon from *Agrobacterium vitis*. *J. Bacteriol.* **177,** 6518–6526
57. Yaoi, T., Miyazaki, K., and Oshima, T. (1997) Substrate recognition of isocitrate dehydrogenase and 3-isopropylmalate dehydrogenase from *Thermus thermophilus*. *J. Biochem.* **121,** 77–81
58. Zhu, G., Golding, G. B., and Dean, A. M. (2005) The selective cause of an ancient adaptation. *Science* **307,** 1279–1282
59. Tipton, P. A. (1993) Intermediate partitioning in the tartrate dehydrogenase-catalyzed oxidative decarboxylation of D-malate. *Biochemistry* **32,** 2822–2827
60. Serfozo, P., and Tipton, P. A. (1995) Substrate determinants of the course of tartrate dehydrogenase-catalyzed reactions. *Biochemistry* **34,** 7517–7524
61. Tawfik, D. S. (2010) Messy biology and the origins of evolutionary innovations. *Nat. Chem. Biol.* **6,** 692–996
62. Wessler, S. R., and Calvo, J. M. (1981) Control of *leu* operon expression in *E. coli* by transcription attenuation mechanism. *J. Mol. Biol.* **149,** 579–597
63. Dean, A. M., and Dvorak, L. (1995) The role of the glutamate 87 in the kinetic mechanism of *Thermus thermophilus* isopropylmalate dehydrogenase. *Protein Sci.* **4,** 2156–2167
64. Gonçalves, S., Miller, S. P., Carrondo, M. A., Dean, A. M., and Matias, P. M. (2012) Induced fit and the catalytic mechanism of isocitrate dehydrogenase. *Biochemistry* **51,** 7098–7115
65. Harding, M. M. (2002) Metal-ligand geometry relevant to proteins and in proteins: sodium and potassium. *Acta Crystallogr. D Biol. Crystallogr.* **58,** 872–874
66. Stokke, R., Madern, D., Fedøy, A. E., Karlsen, S., Birkeland, N. K., and Steen, I. H. (2007) Biochemical characterization of isocitrate dehydrogenase from *Methylococcus capsulatus* reveals a unique NAD$^+$-dependent homotetrameric enzyme. *Arch. Microbiol.* **187,** 361–370